Rotational Excitation of Diatomic Molecules by Slow Electrons: Application to H_2†

NEAL F. LANE* AND S. GELTMAN
Joint Institute for Laboratory Astrophysics, University of Colorado and National Bureau of Standards, Boulder, Colorado
(Received 3 March 1967)

The theory of electron scattering from a rigid rotator is applied to the case of low-energy scattering of electrons from hydrogen molecules in ground electronic and vibrational states. The coupled equations are solved numerically and the resulting S matrix is used to calculate elastic, rotational excitation, and rotational de-excitation cross sections. The electron-molecule interaction potential is based on the approximate charge distribution of H_2 and includes the effects of polarization, which are shown to be important. Cross sections are given for several rotational states, and it is pointed out that while the elastic and inelastic cross sections are found to depend on the initial rotational angular momentum j of the molecule, their variation in j is such that the total cross section remains independent of j. The effects of "back coupling" and coupling with higher rotational states are illustrated by comparing the results of the close-coupling calculation with those of the Born and distorted-wave methods; the distorted-wave and close-coupling results for rotational excitation are found to agree within 20 percent for all energies.

I. INTRODUCTION

THE rotational excitation of diatomic molecules by electron impact has been known for some time to be the dominant energy-loss mechanism for slow electrons in molecular gases.[1] Early theoretical investigations[2,3] of the electron-molecule scattering problem resulted in cross sections far too small to explain the observed energy losses. This was due largely to the neglect of the long-range electron-quadrupole interaction,[4–6] later shown to be primarily responsible for the large rotational-excitation cross sections consistent with the observations.[7,8] Another important contribution to the long-range interaction potential is the so-called polarization interaction, which arises from the induced dipole moment of the molecule.[9] The early calculations were based on the Born approximation, presumed to be valid because of the long-range nature of the interactions. More recent treatments,[10–15] using the method of distorted waves, attempt to also include the short-range electron-molecule interaction, and appear in most cases[10–14] to be in better agreement with the results of the swarm experiments.[7,8] However, the distorted-wave method is still a weak-coupling approximation and neglects, for example, changes in the elastic scattering caused by inelastic processes, thus resulting in violations of particle conservation. These can often be serious, particularly in the heavier molecules, where the interactions are stronger.[14] Another important uncertainty in the electron-molecule scattering problem is the manner of including the *effective* polarization interaction. This is normally accomplished by cutting off the asymptotic form of the potential at some value of r determined by fitting the elastic cross section to either low-energy momentum-transfer measurements,[11] or total cross sections observed at higher energies.[14] The principal objection to the first approach arises from the fact that all partial waves are not affected by the potential in the same way. Hence, adjusting the potential to yield the correct low-energy elastic-scattering cross section, which is primarily due to s-wave scattering, in no way guarantees the correctness of the resulting p-wave scattering, which is found to be most important for rotational excitation. It will, in fact, be shown in the present paper that a change in the interaction potential which gives rise to a 15% change in the rotational-excitation cross section can cause a factor-of-three change in the low-energy elastic scattering. In adjusting the potential to fit total-cross-section measurements at higher energies, however, one must be careful to also consider cross sections for inelastic processes which must be included. Finally, the effect of exchange on the rotational-excitation cross section is not yet known, although it is found to be very important in the case of low-energy elastic scattering.[16]

In the present paper we analyze in detail the scattering of electrons by hydrogen molecules without resorting to the usual weak-coupling approximations. In this way

† This research was supported in part by the Advanced Research Projects Agency (Project DEFENDER), monitored by the U.S. Army Research Office (Durham), under Contract No. DA-31-124-ARO-D-139.

* Visiting Fellow 1965–1966. Present address: Physics Department, Rice University, Houston, Texas.

[1] H. S. W. Massey and E. H. S. Burhop, *Electronic and Ionic Impact Phenomena* (Oxford University Press, London, 1952), p. 278.
[2] P. M. Morse, Phys. Rev. **90**, 51 (1953).
[3] T. R. Carson, Proc. Phys. Soc. (London) **A67**, 909 (1954).
[4] S. Stein, E. Gerjuoy, and I. Holstein, Phys. Rev. **93**, 934 (1954).
[5] E. Gerjuoy and S. Stein, Phys. Rev. **97**, 1671 (1955).
[6] E. Gerjuoy and S. Stein, Phys. Rev. **98**, 1848 (1955).
[7] A. G. Engelhardt and A. V. Phelps, Phys. Rev. **131**, 2115 (1963).
[8] A. G. Engelhardt, A. V. Phelps, and C. G. Risk, Phys. Rev. **135**, A1566 (1964).
[9] A. Dalgarno and R. J. Moffett, Proc. Natl. Acad. Sci. India **A33**, 511 (1963).
[10] R. C. Mjolsness and D. H. Sampson, Phys. Rev. Letters **13**, 812 (1964).
[11] D. H. Sampson and R. C. Mjolsness, Phys. Rev. **140**, A1466 (1965).
[12] K. Takayanagi and S. Geltman, Phys. Letters **13**, 135 (1964).
[13] K. Takayanagi and S. Geltman, Phys. Rev. **138**, A1003 (1965).
[14] S. Geltman and K. Takayanagi, Phys. Rev. **143**, 25 (1966).
[15] A. Dalgarno and R. J. W. Henry, Proc. Phys. Soc. (London) **85**, 679 (1965).
[16] H. S. W. Massey and R. O. Ridley, Proc. Phys. Soc. (London) **A69**, 659 (1956).

we can illustrate the influence of neighboring rotational states on elastic and rotational-excitation cross sections and, in so doing, comment on the reliability of the distorted-wave method. Although we include the polarization in the same rather arbitrary manner as other authors, we are able to obtain good agreement with the total scattering measurements above a few electron volts. Because of the insensitivity of s-wave elastic scattering to the polarization at these energies, we suggest that the p-wave scattering, which is most important to rotational excitation, is well determined within the static-field approximation. In the region of very low energies, the s-wave contribution to the elastic scattering is found to be too large. Massey and Ridley[16] also obtained very large s-wave cross sections in the static-field model which were considerably reduced when exchange was considered, the difference becoming small for energies above 6 eV. In an attempt to simulate the effects of exchange, we modified the static field in the center of the molecule by making it more attractive. As a result, the s-wave cross sections could be reduced to quite reasonable values without appreciably changing the p-wave scattering and, hence, the rotational-excitation cross sections. It is suggested that the effects of exchange on p waves for energies below 5 eV might be expected to be small. Total cross sections, which are found to be relatively independent of the rotational angular momentum, elastic cross sections, and inelastic cross sections are given for several rotational states; and comparisons are made with other theoretical results.

II. THEORY OF ELECTRON-DIATOMIC-MOLECULE SCATTERING

Since the energies of primary interest lie well below the thresholds for electronic and vibrational excitation, we deal only with the rotational structure of the molecule. The polarization of the molecular electronic charge distribution by the scattered electron is represented by means of an effective polarization potential as in the case of previous investigations.[10–14] Only molecular states for which the component of electronic angular momentum along the internuclear axis vanishes, i.e., Σ states, are considered. We neglect the effect of exchange between the scattered and bound electrons. Thus, the molecule is represented by a rigid rotator carrying a polarizable charge distribution. Transitions between rotational states of this rotator are induced by the incident electron through an effective interaction potential which includes the effects of short-range attractive interactions and polarization of the molecular charge cloud, and which asymptotically depends only on the value of the quadrupole moment of the molecule. The complete theory of scattering of an electron by a rigid rotator has been given by Arthurs and Dalgarno.[17] Only essential points in the development will be repeated for purposes of clarity.

[17] A. M. Arthurs and A. Dalgarno, Proc. Roy. Soc. (London) **A256**, 540 (1960).

Consider a system consisting of an electron and a diatomic molecule, which we are representing by a rigid rotator having momenta of inertia I. The total Hamiltonian in the center-of-mass system may be written (we shall use atomic units throughout):

$$H=H_R-(1/2\mu)\nabla_{\mathbf{r}}^2+V(\mathbf{r},\hat{s}), \tag{1}$$

where H_R is the rotational Hamiltonian of the molecule, $-(1/2\mu)\nabla_{\mathbf{r}}^2$ is the kinetic-energy operator for the scattered electron, $V(\mathbf{r},\hat{s})$ is the electron-molecule effective interaction potential, and $\mathbf{r}$ and $\hat{s}$ denote the coordinates of the electron and the orientation of the internuclear axis, respectively. The wave functions describing the rotational states of the molecule are, in the rigid-rotator approximation, the familiar spherical harmonics $Y_{jm_j}(\hat{s})$ which satisfy

$$[H_R-j(j+1)/2I]Y_{jm_j}(\hat{s})=0, \tag{2}$$

where $\mathbf{j}$ is the rotational angular momentum and m_j, its component along the z axis.

It is found convenient to couple the angular momentum $\mathbf{j}$ of the molecule with that of the projectile electron $\mathbf{l}$ in order to form the total angular momentum $\mathbf{J}=\mathbf{j}+\mathbf{l}$ of the system and its component $M=m_j+m_l$ along the z axis. Total wave functions, which are also eigenfunctions of J^2 and J_z, are found to satisfy

$$(H-E_j)\psi_{jl}^{JM}(\mathbf{r},\hat{s})=0, \tag{3}$$

where j and l specify the initial angular momentum of the molecule and electron, respectively, and where E_j is the total energy.

Constructing appropriate basis functions

$$\mathcal{Y}_{jl}^{JM}(\hat{r},\hat{s})=\sum_{m_j}\sum_{m_l}(jlm_jm_l|jlJM)\,Y_{jm_j}(\hat{s})\,Y_{lm_l}(\hat{r}), \tag{4}$$

the coefficients being the familiar Clebsch-Gordan or vector-coupling coefficients, we expand in terms of this set:

$$\Psi_{jl}^{JM}(\mathbf{r},\hat{s})=\sum_{j'}\sum_{l'}r^{-1}u_{j'l'}^{Jjl}(r)\mathcal{Y}_{j'l'}^{JM}(\hat{r},\hat{s}), \tag{5}$$

where the radial coefficients $u_{j'l'}^{Jjl}(r)$ may be shown to satisfy the set of coupled equations

$$[(d^2/dr^2)+k_{j'}^2-l'(l'+1)/r^2]u_{j'l'}^{Jjl}(r)$$
$$=\sum_{j''}\sum_{l''}\langle j'l';J\,|\,V\,|\,j''l'';J\rangle u_{j''l''}^{Jjl}(r), \tag{6}$$

where $k_{j'}^2=k_j^2-2B_0[j'(j'+1)-j(j+1)]$, and $B_0=1/2I$ is the molecular rotational constant in atomic units.

The matrix elements appearing in the coupled equations are given by

$$\langle j'l';J\,|\,V\,|\,j''l'';J\rangle=2\iint\mathcal{Y}_{j'l'}^{JM*}V\mathcal{Y}_{j''l''}^{JM}d\hat{r}d\hat{s}, \tag{7}$$

where, upon expansion of the axially symmetric potential as

$$V(\mathbf{r},\hat{s})=\sum_{\lambda} v_\lambda(r)P_\lambda(\hat{r}\cdot\hat{s}), \tag{8}$$

we obtain

$$\langle j'l';J\,|\,V\,|\,j''l'';J\rangle=\sum_{\lambda} v_\lambda(r)f_\lambda(j'l',j''l';J), \tag{9}$$

where

$$f_\lambda(j'l',j''l';J)=(-1)^{j'+j''-J}(2\lambda+1)^{-1}[(2j'+1)(2l'+1)(2j''+1)(2l''+1)]^{1/2}\times(l'l''00\,|\,l'l''\lambda0)(j'j''00\,|\,j'j''\lambda0)W(j'l'j''l'';J\lambda), \tag{10}$$

W being the familiar Racah coefficient.[18] Since we are considering the case of homonuclear diatomic molecules, only even values of λ will appear in the expansion of V. The f_λ are known to vanish unless the following conditions[19] are satisfied:

$$|j'-j''|\leq\lambda\leq j'+j'',$$
$$|l'-l''|\leq\lambda\leq l'+l'',$$

$j'+j''+\lambda$ and $l'+l''+\lambda$, even,

$$(-1)^{j'+l'}=(-1)^{j''+l''}.$$

The requirement that the functions $u_{j'l'}{}^{Jjl}(r)$ behave asymptotically as

$$u_{j'l'}{}^{Jjl}(r)\sim\delta_{jj'}\delta_{ll'}\exp[-i(k_jr-l\pi/2)]-(k_j/k_{j'})^{1/2}S^J(j'l',jl)\exp[i(k_{j'}r-l'\pi/2)], \tag{11}$$

specifies the relationship between elements of the S matrix and the cross sections for $j\to j'$ transitions averaged over all m_j and summed over all $m_{j'}$. We obtain

$$\sigma(j',j)=[\pi/(2j+1)k_j^2]\sum_{J=0}^{\infty}\sum_{l}\sum_{l'}(2J+1)\,|\,T^J(j'l',jl)\,|^2, \tag{12}$$

where

$$\mathbf{T}=\mathbf{1}-\mathbf{S}, \tag{13}$$

and where l and l' take on all values consistent with j, j', and J. In writing Eqs. (11) and (12), we have made use of the fact, which may be easily demonstrated, that $\mathbf{S}$ is diagonal in J and independent of M. It is often convenient, particularly in numerical treatments, to deal only with real solutions of the coupled equations, in which case it is well known that asymptotic conditions of the form[20]

$$u_{j'l'}{}^{Jjl}(r)\sim\delta_{jj'}\delta_{ll'}\cos(k_jr-l\pi/2)+(k_j/k_{j'})^{1/2}R^J(j'l',jl)\sin(k_{j'}r-l'\pi/2) \tag{14}$$

lead to a relation between the R and S matrices given by

$$\mathbf{S}=(\mathbf{I}+i\mathbf{R})(\mathbf{I}-i\mathbf{R})^{-1}=[(\mathbf{I}-\mathbf{R}^2)+2i\mathbf{R}](\mathbf{I}+\mathbf{R}^2)^{-1}, \tag{15}$$

where the R matrix is real and symmetric. Fundamental to this treatment of the scattering problem is the fact that the S matrix is unitary and symmetric.[21] The symmetry property of the S matrix is a statement of detailed balancing and allows us to relate cross sections for inverse processes by the relation

$$k_j^2(2j+1)\sigma(j',j)=k_{j'}^2(2j'+1)\sigma(j,j'). \tag{16}$$

III. THE METHOD OF CALCULATION

The problem of calculating cross sections for rotational excitation and elastic scattering within the framework set out in the previous discussions simply reduces to that of solving the set of coupled Eqs. (6) subject to the asymptotic conditions of Eq. (14). The method follows generally that of Barnes, Lane, and Lin.[20]

We rewrite the coupled equations as

$$\left(\frac{d^2}{dr^2}\right)y_{\mu\nu}=\sum_{\gamma=1}^{N_c}G_{\mu\gamma}y_{\gamma\nu}, \tag{17}$$

where

$$G_{\mu\gamma}=U_{\mu\gamma}-k_\mu^2\delta_{\mu\gamma}+l_\mu(l_\mu+1)\delta_{\mu\gamma}/r^2, \tag{18}$$

$$U_{\mu\gamma}=2\sum_{\lambda} v_\lambda(r)f_\lambda(j_\mu l_\mu,j_\gamma l_\gamma;J), \tag{19}$$

and where μ designates a component of the solution, and ν denotes one of the N_c linearly independent solutions which vanish at $r=0$ (N_c being the total number of channels). The equivalent matrix equation is

$$((d^2/dr^2)-\mathbf{G})\mathbf{y}=0. \tag{20}$$

To accomplish the numerical integration of this equation, we employ the Numerov method which is based on the finite-difference relation[22]

$$\delta^2\mathbf{y}=(\delta r)^2\tfrac{1}{12}[\mathbf{y}''+\delta^2(\mathbf{y}'')], \tag{21}$$

where

$$\delta^2(\mathbf{y})=\mathbf{y}_{n+1}-2\mathbf{y}_n+\mathbf{y}_{n-1},$$
$$\delta r=r_{n+1}-r_n,$$
$$\mathbf{y}''=(d^2/dr^2)\mathbf{y},$$

and where $\mathbf{y}_n=\mathbf{y}(r_n)$, n labeling a particular point in the integration mesh. Combining Eqs. (20) and (21),

[18] G. Racah, Phys. Rev. **62**, 438 (1942); L. C. Biedenharn, J. M. Blatt, and M. E. Rose, Rev. Mod. Phys. **24**, 249 (1952).
[19] I. C. Percival and M. J. Seaton, Proc. Cambridge Phil. Soc. **53**, 654 (1957).
[20] L. L. Barnes, N. F. Lane, and C. C. Lin, Phys. Rev. **137**, A388 (1965).
[21] J. M. Blatt and L. C. Biedenharn, Rev. Mod. Phys. **24**, 258 (1952).
[22] D. R. Hartree, *The Calculation of Atomic Structures* (John Wiley & Sons, Inc., New York, 1957), p. 71.

we obtain the generalized Numerov algorithm

$$\mathbf{y}_{n+1}=[\mathbf{I}-\tfrac{1}{12}(\delta r)^2\mathbf{G}_{n+1}]^{-1}\{[2\mathbf{I}+\tfrac{5}{6}(\delta r)^2\mathbf{G}_n]\mathbf{y}_n - [\mathbf{I}-\tfrac{1}{12}(\delta r)^2\mathbf{G}_{n-1}]\mathbf{y}_{n-1}\}, \quad (22)$$

where

$$\mathbf{G}_n=\mathbf{G}(r_n).$$

Thus, once the solution is specified at two points, it may be extended to arbitrary values of r by means of this formula.

It is clear from Eq. (22) that the second index of the solution $\mathbf{y}$ remains untouched by the coupling. Thus, we develop, simultaneously, N_c separate vector solutions of Eq. (20), each particular solution being labeled by the second index. In order that we may eventually combine these solutions to obtain those appropriate to the physical problem, i.e., those having the correct asymptotic form, we require that they be linearly independent. To begin the integration, we make use of the fact that for small values of r

$$G_{\mu\gamma}\rightarrow l_\mu(l_\mu+1)\delta_{\mu\gamma}/r^2, \quad (23)$$

and therefore

$$y_{\mu\nu}\rightarrow r^{l_\mu+1}\alpha_{\mu\nu}, \quad (24)$$

where, in order to guarantee linearly independent solutions, $\boldsymbol{\alpha}$ is required to be nonsingular.

Because of the arbitrary choice for $\boldsymbol{\alpha}$, the solutions $\mathbf{y}$ will not be the $\mathbf{u}$ of Sec. II in that they will not have the same asymptotic behavior. However, for r sufficiently large, we may write

$$\mathbf{y}\sim\mathbf{B}_1\mathbf{A}+\mathbf{B}_2\mathbf{B}, \quad (25)$$

where

$$(B_1)_{\mu\nu}=\delta_{\mu\nu}(k_\mu r)j_{l_\mu}(k_\mu r),$$
$$(B_2)_{\mu\nu}=-\delta_{\mu\nu}(k_\mu r)n_{l_\mu}(k_\mu r).$$

The functions j_{l_μ} and n_{l_μ} are spherical Bessel functions of the first and second kind, respectively,[23] and $\mathbf{A}$ and $\mathbf{B}$ are constant matrices, which may be determined by matching $\mathbf{y}$ to the asymptotic form of Eq. (25) at two large values of r, say r_a and r_b. We obtain

$$\mathbf{A}=\mathbf{D}^{-1}[(\mathbf{B}_2)_b\mathbf{y}_a-(\mathbf{B}_2)_a\mathbf{y}_b] \quad (26)$$

and

$$\mathbf{B}=-\mathbf{D}^{-1}[(\mathbf{B}_1)_b\mathbf{y}_a-(\mathbf{B}_1)_a\mathbf{y}_b], \quad (27)$$

where

$$\mathbf{D}=[(\mathbf{B}_2)_b(\mathbf{B}_1)_a-(\mathbf{B}_2)_a(\mathbf{B}_1)_b], \quad (28)$$

and where $(\mathbf{B}_1)_a$ represents the diagonal matrix $\mathbf{B}_1$ evaluated at $r=r_a$. Defining diagonal matrices for the electron momenta, viz.,

$$K_{\mu\nu}=\delta_{\mu\nu}k_\mu, \quad (29)$$

it may easily be shown that

$$\mathbf{R}=\mathbf{K}^{1/2}(\mathbf{B}\mathbf{A}^{-1})\mathbf{K}^{-1/2}, \quad (30)$$

the relation between the R and S matrices having been defined in Sec. II.

A main program organizes the input information, initializes the subroutines, and calls on them individually to assign values of j_μ, l_μ, and k_μ^2 to each channel μ. The matrix elements $U_{\mu\gamma}$ are then calculated and the coupled equations integrated to obtain the solutions $y_{\mu\gamma}$. These solutions are then matched asymptotically as in Eq. (25) and the matrices $\mathbf{A}$ and $\mathbf{B}$ determined. These are used to calculate the R and S matrices which yield cross sections for all possible processes involving the rotational states considered. As part of the input information, one specifies the short-range field of the molecule in numerical form, the polarizabilities, quadrupole moment, rotational constant and various parameters which define the precise forms of the long-range part of the interaction potential, that is, all information characteristic of the particular molecule under investigation. In addition, it is necessary to specify the total number of rotational states N to be considered simultaneously. Except for the integration and boundary matching data, the remainder of the input information consists of the smallest rotational angular momentum j_1 to be considered, the incident kinetic energy k_1^2 of the electron with the molecule in the rotational state j_1, the total angular momentum J of the system, and the parity p. The coefficients $f_\lambda(j_\mu l_\mu, j_\nu l_\nu; J)$, which are entirely responsible for the coupling of channels μ and ν, vanish unless $j_\mu+l_\mu$ and $j_\nu+l_\nu$ are of the same parity, i.e.,

$$(-1)^{j_\mu+l_\mu}=(-1)^{j_\nu+l_\nu}.$$

Thus, the original set of coupled equations splits into two smaller sets, completely independent of one another, which may conveniently be handled separately. We find it convenient to include J in the definition of the parity, viz.,

$$p=0\ (1) \qquad \text{for even (odd)} \quad j_\mu+l_\mu+J. \quad (31)$$

The total number of channels can be reduced significantly by ignoring all values of $l>5$; this is found to be a very good approximation for energies in the range of interest. As was mentioned previously, the rotational-excitation cross sections for energies, of say less than 1 eV, are found to come mainly from $p\rightarrow p$ and to a lesser extent from $s\rightarrow d$ and $d\rightarrow s$ transitions. Therefore it follows from the properties of the f_λ coefficients that for the rotational transition $j=1\rightarrow j'=3$, only $p=0$ and $J=1$, 2, and 3 will contribute significantly; the other values of J may generally be ignored within an accuracy of 1 percent. Clearly, for the transition $j=3\rightarrow j'=5$, the important total angular momentum values are $J=3$, 4, and 5; and for transitions between higher-rotational states, the important values of J are correspondingly higher.

The numerical integration was performed over different choices of step size depending on the energy. Typical choices of the integration mesh are given by: $r=0.001$ to 0.01 a_0 in steps of 0.001 and $r=0.01$ to 3.0 a_0 in steps of 0.02. The small step size in the latter region was chosen to ensure proper handling of the peaked behavior of $v_2(r)$ and $v_4(r)$ in the region $r\approx s/2$.

[23] *Handbook of Mathematical Functions*, edited by M. Ambramowitz and I. A. Stegun, Appl. Math. Ser. 55 (U.S. Department of Commerce, National Bureau of Standards, Washington, D.C., 1964), p. 437.

Step sizes used in the region $r>3.0\ a_0$ varied with the energy, typical cases being 0.5 a_0 for $k^2 \lesssim 0.01$ Ry, 0.2 a_0 for $0.01 \lesssim k^2 \lesssim 0.1$ Ry, and 0.1 a_0 for $k^2>0.1$ Ry. Calculations have been made using a finer mesh for checking purposes. The integration procedure was checked directly by setting all $v_\mu(r)=0$ and comparing the results with appropriately scaled spherical Bessel functions. For values of $l<5$ the error was completely negligible, while for $l=5$ it was of the order of 1 percent. For values of $l>5$ the errors were much greater; however, we did not find it necessary to include these larger l in any of the calculations reported below. In regard to errors in the solutions of the coupled equations, we may obtain a good measure of accuracy by observing the symmetry of the R and S matrices resulting from the boundary matching. This symmetry property, although guaranteed theoretically, will be destroyed by errors in the numerical integration or boundary matching. The low-energy results tend to show less symmetry, since one must integrate to large values of r in order to determine the R and S matrices, and in doing so a larger number of steps is involved. It should be emphasized that symmetry of the R matrix is only a measure of the accuracy of the wave functions and does not guarantee that the functions are in the asymptotic region where the correct R and S matrices may be determined. This is ascertained by matching at several points and observing the convergence of the variable R matrix, obtained in this way, toward a constant value. In our calculations, the number of significant figures of symmetry in the S-matrix ranges from three for $k^2=0.004$ Ry to five for $k^2=0.09$ Ry and more for higher energies. The Racah coefficients calculated for use in the f_μ and the spherical Bessel functions used in the boundary matching were checked against existing tables and formulas for a wide variety of parameters.

IV. ELECTRON SCATTERING WITH MOLECULAR HYDROGEN

Hydrogen, being the simplest of neutral diatomic molecules, is a particularly good choice to illustrate the details of the close coupling calculation (since we are able to represent the electron-molecule static interaction potential with a greater degree of certainty than in the case of the heavier molecules). However, in the case of H_2, the neglect of exchange, which is inherent in our calculation, is very likely to be important and in fact could be critical in determining the correct scattering length; we will discuss this point further in connection with results of the calculations.

The simple H_2 wave function of Wang[24] may be written

$$\psi(\mathbf{r}_1, \mathbf{r}_2) = C\{\exp[-Z(r_{1a}+r_{2b})]+\exp[-Z(r_{1b}+r_{2a})]\}, \tag{32}$$

where the radial distances of the two electrons from one nucleus, say nucleus a, are given by r_{1a} and r_{2a},

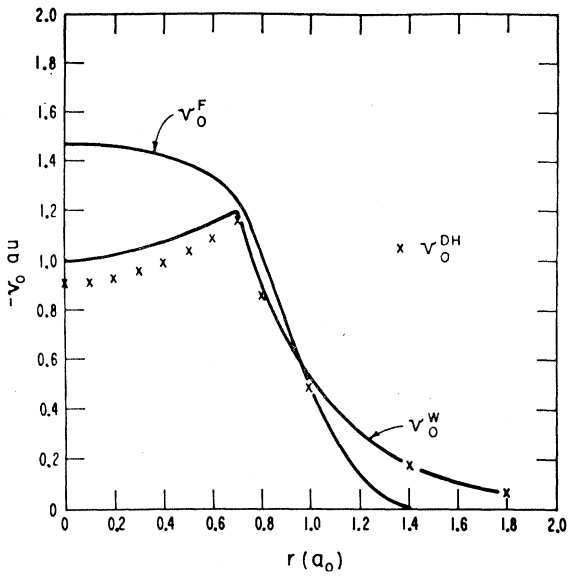

FIG. 1. Comparison of spherical terms in the interaction potential resulting from the Wang function (W), used by Dalgarno and Henry (DH), and calculated from the potential given by Fisk (F).

and from the other nucleus by r_{1b} and r_{2b}. The value of the effective charge was determined variationally to be $Z=1.166$, giving for the internuclear separation $s=1.406\ a_0$ and for the ground-state energy $E_0=-2.278$ Ry. Adopting this wave function and ignoring the cross terms in $|\psi|^2$ in calculating the electron-molecule interaction potential, we find that the electron-molecule interaction averaged over the molecular ground-state wave function becomes

$$V(\mathbf{r}) = v(r_a)+v(r_b), \tag{33}$$

where

$$v(r_a) = -(1.166+1/r_a)\exp(-2.332r_a), \tag{34}$$

and similarly for $v(r_b)$, r_a and r_b being the distances of the scattered electron from the two nuclei. The cross terms in $|\psi|^2$ would have the effect of increasing slightly the value of $v_\mu(r)$ in the region between the nuclei (see Fig. 1). However, we cannot hope to represent the potential accurately in this region, and the small error introduced in this way is of little consequence. Expanding $V(\mathbf{r})$ in a series of Legendre polynomials as in Eq. (8), one obtains the coefficient functions $v_0^W(r)$, $v_2^W(r)$, and $v_4^W(r)$ illustrated in Figs. 1 and 2. Also given for comparison are the coefficients $v_\mu^{DH}(r)$ used by Dalgarno and Henry[15] in their distorted-wave calculation of rotational excitation in H_2. They employed the one-center wave function of Hagstrom and Shull,[25] which included several configurations, and obtained analytic expressions for the $v_\mu^{DH}(r)$. For purposes of comparison, we have also included in Figs. 1 and 2, the coefficients $v_\mu^F(r)$ obtained by expanding in a series of Legendre polynomials the potential func-

[24] S. C. Wang, Phys. Rev. **31**, 579 (1928).

[25] S. Hagstrom and H. Shull, J. Chem. Phys. **30**, 1314 (1959).

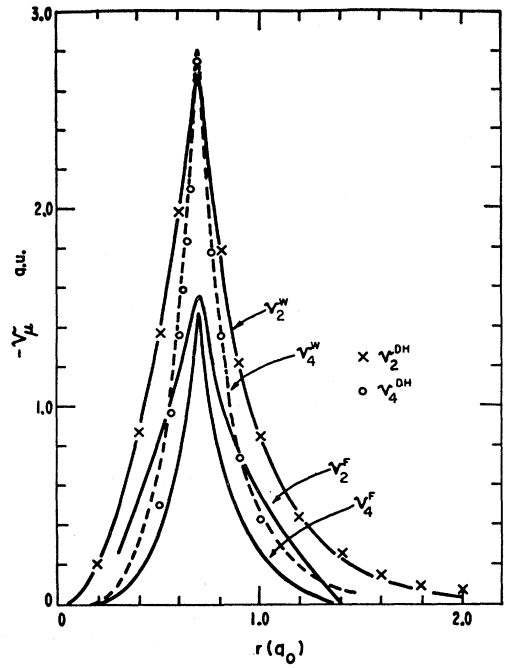

FIG. 2. Comparison of the $v_2(r)$ and $v_4(r)$ coefficients in the interaction potential resulting from the Wang function (W), used by Dalgarno and Henry (DH), and calculated from the potential given by Fisk (F).

tion used by Fisk[26] in calculating elastic scattering of electrons by diatomic molecules. These coefficients have been used more recently by Oksyuk[27] in connection with the "adiabatic approximation" to calculate rotational- and vibrational-excitation cross sections of diatomic molecules. The Fisk potential was not calculated by using actual molecular wave functions, but rather was constructed in a manner similar to that of Allis and Morse in the case of atoms.[28] We shall discuss this work again later in this section. The agreement between the v_μ^{W} and v_μ^{DH} suggests that the average electron-molecule interaction potential is not very sensitive to the choice of molecular wave function. The $v_\mu^{\mathrm{DH}}(r)$ possess the advantage that for large separations

$$v_2^{\mathrm{DH}}(r)\sim -Q/r^3, \tag{35}$$

which is the correct asymptotic behavior for the static field. [Dalgarno and Henry[15] used the value $Q=0.473$ instead of the value $Q=0.49$ adopted by us. Thus, in Fig. 2, their values for $v_2^{\mathrm{DH}}(r)$ should for comparison be increased slightly by a variable factor approaching $0.49/0.473\equiv 1.04$ for $r\to\infty$ 118, 119.] Our choice of molecular wave function, however, results in exponential behavior for all the $v_\mu(r)$ asymptotically. In order, then, to guarantee the correct asymptotic behavior of our interaction potential, we add to the short-range potentials $v_\mu^{\mathrm{W}}(r)$, the long-range (LR) electron quadrupole interaction, and effective polarization interactions given together by

$$v_{\mathrm{LR0}}(r)=-(\alpha/2r^4)C(r), \tag{36}$$

$$v_{\mathrm{LR2}}(r)=-(\alpha'/2r^4+Q/r^3)C(r), \tag{37}$$

where the spherical and nonspherical polarizabilities are taken to be $\alpha=5.5\ a_0^3$ and $\alpha'=1.38\ a_0^3$, respectively,[11,29] where the quadrupole moment is $Q=0.49e\ a_0^2$,[11] and where the function

$$C(r)=1-\exp[-(r/R)^p] \tag{38}$$

removes these long-range forms near the molecule. The value $p=6$, which we use throughout the investigation, results in a rather sharp cutoff for $r\leq R$. Typical values of R range from 1.4 to 2.0 a_0. Thus we assume for the interaction potential of Eq. (8), the form

$$V(\mathbf{r},\hat{s})=\sum_{\mu=0}^{4} v_\mu(r)P_\mu(\hat{r}\cdot\hat{s}), \tag{39}$$

where

$$\begin{aligned} v_0(r)&=v_0^{\mathrm{W}}(r)+v_{\mathrm{LR0}}(r),\\ v_2(r)&=v_2^{\mathrm{W}}(r)+v_{\mathrm{LR2}}(r), \end{aligned} \tag{40}$$

and

$$v_4(r)=v_4^{\mathrm{W}}(r).$$

The quadrupole moment and nonspherical polarizability are both positive in the case of H_2 and come into the interaction potential with the same symmetry. Hence, their effects on the contribution to elastic and inelastic scattering coming from intermediate values of r, i.e., $r\gtrsim R$, will be much the same. Since the polarization interaction must be truncated at small r in a rather arbitrary manner, the similar treatment of the quadrupole interaction, although somewhat undesirable, is not a serious limitation. We will see, in comparing calculated and observed total cross sections, that reasonable values of R may be chosen to give agreement over a good portion of the energy range of measurement.

In order to illustrate several features of the problem, we arbitrarily choose a value of $R=s=1.40\ a_0$, which is quite reasonable, since $R=1.4\ a_0$ is outside the region in which the short-range interactions are seen to be large (see Figs. 1 and 2). The effect on elastic and inelastic cross sections of coupling between different rotational states as well as the convergence of these cross sections when the number of states considered is increased can be deduced from the results given in Table I. The $j=1\to 3$ inelastic and $j=1$ elastic cross sections, denoted, respectively, by $\sigma(3,1)$ and $\sigma(1,1)$, are given for several energies and several choices of N, the number of rotational states included in the expansion of the total wave function in Eq. (5). The greatest change in $\sigma(1,1)$ is seen to occur in going from $N=1$

[26] J. B. Fisk, Phys. Rev. **49**, 167 (1936).
[27] Y. D. Oksyuk, Zh. Eksperim. i Teor. Fiz. **49**, 1261 (1966). [English transl.: Soviet Phys.—JETP **22**, 873 (1966)].
[28] W. P. Allis and P. M. Morse, Z. Physik **70**, 567 (1931).
[29] N. J. Bridge and A. D. Buckingham, J. Chem. Phys. **40**, 2733 (1964).

TABLE I. Convergence of H_2 elastic $\sigma(1,1)$ and inelastic $\sigma(3,1)$ cross sections, in units of a_0^2, in N (the number of states) for the case $R=1.4\ a_0$.

k^2 (Ry) / N	0.03		0.06		0.09		0.3		0.6	
	$\sigma(3,1)$	$\sigma(1,1)$	$\sigma(3,1)$	$\sigma(1,1)$	$\sigma(3,1)$	$\sigma(1,1)$	$\sigma(3,1)$	$\sigma(1,1)$	$\sigma(3,1)$	$\sigma(1,1)$
1	•••	55.80	•••	59.30	•••	62.43	•••	73.59	•••	58.03
2	0.541	50.21	1.511	56.04	3.077	62.22	10.07	73.27	5.123	52.53
3	0.580	49.72	1.661	55.76	3.452	62.25	10.82	72.67	5.350	52.21
4	0.582	49.72	1.667	55.77	3.468	62.26	10.84	72.64	5.357	52.19

to $N=2$, as is expected, since here an inelastic channel is introduced which is expected to have a considerable effect on the amount of outgoing flux in the elastic channel. Examining the partial cross sections, we have found that at the lower energies the elastic scattering is primarily s wave ($l=0\rightarrow l'=0$), the p-wave ($l=1\rightarrow l'=1$) contribution becoming comparable for $k^2\gtrsim 0.3$ Ry. Both the s- and p-wave scattering are considerably influenced by the coupling with d- and p-wave channels, respectively, in the $j=3$ rotational state. Partial cross sections for $l\geq 2$ are quite insensitive to the coupling. The convergence of $\sigma(3,1)$ and $\sigma(1,1)$ with increasing N is clearly demonstrated by comparing the $N=2$, 3, and 4 results.

The low-energy electron-molecule scattering problem has the inherent advantage that each additional rotational state considered has associated with it a correspondingly larger angular momentum j. Thus, for example, in the case of $\sigma(3,1)$ the $p\rightarrow p$ transition is the dominant contributor and occurs for a total angular momentum $J=2$. The further inclusion of states $j=5$ and 7 gives rise to coupling with $l=3$ and 5 channels, respectively, resulting in only small changes in the cross section. Higher-rotational states are associated with correspondingly larger values of l for $J=2$, and the effect of including them becomes negligible. In order to check the previous remark, cross sections were calculated in the $N=2$ and $N=3$ schemes while leaving out the $l=5$ channels; the differences for all partial cross sections and for all energies considered were less than 1%.

In this same model, viz., $R=1.4\ a_0$, the j dependence of the elastic $\sigma(j,j)$, inelastic $\sigma(j',j)$, and total $\sigma_T(j)$ cross sections was examined. We define the total cross section by the relation

$$\sigma_T(j)=\sigma(j,j)+\sigma(j+2,j)+\sigma(j-2,j), \quad (41)$$

the last term being zero for $j=0$ and 1; we are temporarily ignoring cross sections for $j\rightarrow j\pm 4$ transitions, which are found to be quite small. In Table II cross sections are given for several values of j. It is interesting to note that while the inelastic cross sections consistently decrease with increasing j, the elastic cross sections increase in going from $j=0$ to $j=1$ and then appear to approach a constant value for larger values of j where the superelastic cross sections begin to contribute. The net result is that the total cross section remains rather insensitive to the value of j considered. Insensitivity of the *elastic* cross section to j has been discussed in some detail by Arthurs and Dalgarno,[17] who show that in cases where the nonspherical part of the interaction may be taken as a perturbation to the spherical part, the first-order contribution of these "orientation-dependent" terms to the *elastic* cross section vanishes for all values of l with the result that the *elastic* cross section remains quite insensitive to j. In our case the nonspherical part of the interaction is not particularly small compared to the spherical part (see Figs. 1 and 2), and the elastic cross section does show some j dependence. The insensitivity of the *total* cross section to j is, however, somewhat striking. Oksyuk,[27] in his application of the adiabatic approximation to the

TABLE II. Comparison of H_2 elastic $\sigma(j,j)$, inelastic $\sigma(j',j)$, and total $\sigma_T(j)$ cross sections in units of a_0^2 calculated with $R=1.4\ a_0$ and $N=3$. The total cross section $\sigma_T(3)$ includes the superelastic cross section $\sigma(1,3)$.

k^2 (Ry) / j',j	0.03	0.06	0.09	0.3	0.6	0.9	1.2	1.5
0, 0	49.24	54.50	59.72	65.43	48.66	38.44	31.52	26.70
1, 1	49.72	55.76	62.25	72.67	52.21	40.43	32.84	27.68
3, 3	49.92	55.55	61.39	70.72	51.32	39.88	32.43	27.33
2, 0	1.062	2.920	5.956	18.050	8.908	5.000	3.303	2.445
3, 1	0.580	1.661	3.452	10.815	5.350	3.003	1.984	1.469
5, 3	0.354	1.093	2.307	8.024	4.093	2.304	1.520	1.124
1, 3	0.368	0.901	1.747	4.670	2.284	1.282	0.846	0.627
$\sigma_T(0)$	50.30	57.42	65.68	83.48	57.57	43.44	34.82	29.15
$\sigma_T(1)$	50.30	57.42	65.70	83.48	57.56	43.43	34.82	29.15
$\sigma_T(3)$	50.64	57.54	65.44	83.41	57.70	43.47	34.80	29.08

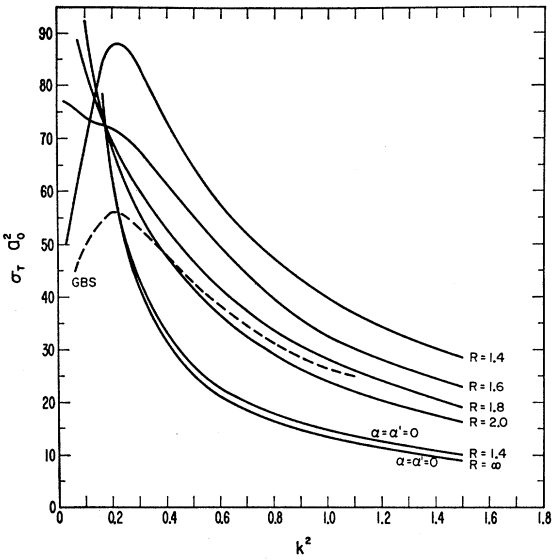

FIG. 3. Calculated values of the total cross section (in a_0^2) versus the initial electron energy (in rydberg units) for values of the long-range cutoff radius (in a_0): $R=1.4$, 1.6, 1.8, 2.0, 1.4 ($\alpha=\alpha'=0$) and ∞ ($\alpha=\alpha'=0$); recent measurements by Golden, Bandel, and Salerno (GBS) of the total electron-H_2 cross section.

electron-molecule scattering, has obtained the result

$$\sum_{j'} \sigma(j',j) = \text{const}, \tag{42}$$

which is in agreement with our observations.

The previous discussion has been in reference to a particular model in which the cutoff radius for the long-range field R was taken to be 1.4 a_0. In carrying out similar calculations with other values of R, it is found, however, that the general behavior of the cross sections as regards their dependence on the number of states included and on the particular j values considered is the same. In Fig. 3 calculated total cross sections for several values of R are compared with the most recent total cross-section measurements of Golden *et al.*[30] Also given for reference are cross sections calculated with the polarization completely neglected; in this case the effect of R is simply to cut off the quadrupole interaction, and the dependence is seen to be weak. In comparing our calculated total cross sections with the experimental results, we make use of the fact that cross sections for vibrational and electronic excitation are observed to be small throughout the range of energies considered.[8,31] It is clear from Fig. 3 that for energies above a few electron volts, it is necessary to include a certain amount of the polarization interaction in order to obtain total cross sections in reasonable agreement with experiment. The values of the cutoff parameter $R=1.8$ a_0 and $R=2.0$ a_0 seem to yield the most reasonable results for these larger energies. For smaller energies, however, the partial cross section corresponding to $l=0\rightarrow l'=0$ becomes large. This occurs also in the cases where $\alpha=\alpha'=0$, corresponding to use of the short-range static field alone ($R=\infty$), or in cases with the quadrupole tail ($R=1.4$ a_0). Since, in the latter case, our interaction is in such close agreement with that of Dalgarno and Henry (see Figs. 1 and 2), we would expect the curve corresponding to $\alpha=\alpha'=0$ and $R=1.4$ a_0 to represent a total cross section appropriate to their calculations. The failure to obtain reasonable low-energy cross sections is not surprising when one considers the sensitivity of the s-wave scattering at low energies to changes in the interaction potential in the region of the center of the molecule, as will be discussed below. However, this inability to represent s-wave scattering correctly does not necessarily imply that the calculated rotational excitation cross sections are also poorly defined. The variation in R of partial cross sections contributing to the elastic cross section for $j=0$ is illustrated in Fig. 4. For energies greater than a few electron volts, the $s\rightarrow s$ contribution $\sigma_0(0,0)$ is seen to be rather insensitive to changes in R, while the corresponding $p\rightarrow p$ contribution $\sigma_1(0,0)$ changes appreciably with variations in R and is responsible for the R sensitivity felt in the total cross section. This property is found to hold for other values of j as well.

The symmetry of the interaction potential, as given

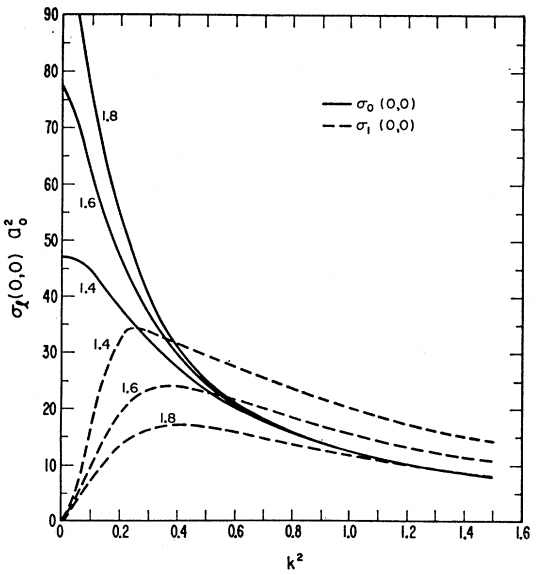

FIG. 4. Comparison of the sensitivity of the elastic s- and p-wave partial cross sections (in a_0^2) to the long-range cutoff radius R ($R=1.4$, 1.6, and 1.8 a_0) for scattering in the $j=0$ rotational state.

[30] D. E. Golden, H. W. Bandel, and J. A. Salerno, Phys. Rev. **146**, 40 (1966).
[31] G. J. Schulz, Phys. Rev. **135**, A988 (1964).

in Eq. (8), is such that $l=0\rightarrow l'=0$ offers no coupling and, hence, makes no contribution to the cross section for transitions between different rotational states. Of the transitions contributing, viz. $l=0\rightarrow l'=2$, $l=2\rightarrow l'=0$, $l=2\rightarrow l'=2$ and $l=1\rightarrow l'=1$, only two are important at the energies of interest here. Very close to threshold the energy in the outgoing channel is so small as to allow only outgoing s waves, with the result that the $d\rightarrow s$ contribution is dominant for energies of say up to 0.02 eV above threshold. At slightly higher energies the $p\rightarrow p$ contribution takes over and remains the principal contributor throughout the entire energy range considered here, i.e., up to about 20 eV. The p-wave functions, because of the presence of an effective potential barrier $2/r^2$, are of course much less penetrating than s-wave functions and are sensitive to changes in the intermediate and long-range part of the interaction potential. The long-range character is more important at low energies where sensitivities are reflected in the rotational-excitation cross sections as illustrated in Fig. 5. Here the inelastic cross section $\sigma(2, 0)$ corresponding to the $j=0\rightarrow j'=2$ transition is given as a function of energy for several choices of the long-range part of the interaction. As one would expect, the quadrupole moment is extremely important at low energies and in fact determines the threshold behavior completely. It is interesting to note, in addition, that its effects are also felt at energies approaching 20 eV. The polarization interaction, which is also seen to be important, introduces into the cross section most of the dependence on the cutoff radius R. The differences, however, in the cross sections resulting from the two most reasonable choices of $R=1.8$ and 2.0 a_0 are less than 12% for energies less than 0.4 eV and are never larger than about 40%. The larger differences occur at intermediate energies where the p-wave functions have their maximum overlap with the interaction potential in the region of the long-range cutoff. At the higher energies the cross sections become somewhat independent of the choice of R as the p-wave functions begin to penetrate the short-range field.

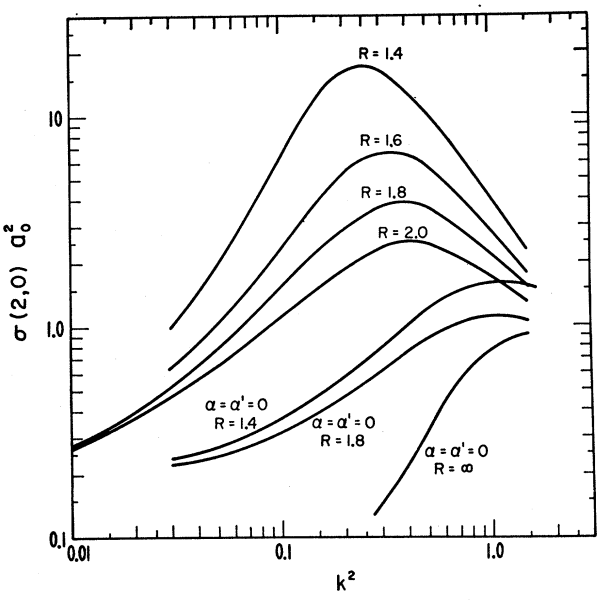

FIG. 5. The rotational excitation cross section $\sigma(2, 0)$ versus energy (in rydberg units) calculated for several choices $R=1.4$, 1.6, 1.8, and 2.0 of the long-range cutoff radius (in a_0) and $\alpha=\alpha'=0$, $R=1.4$, 1.8, and ∞.

In order to investigate the sensitivity of the cross sections to changes in the short-range part of the potential, we modified the short-range potential by a multiplicative factor of the form

$$B(r)=\exp[-B(s/2-r)], \qquad r\leq\tfrac{1}{2}s,$$
$$=1, \qquad r>\tfrac{1}{2}s. \tag{43}$$

Hence, the modified interaction potential is given by

$$V^B(\mathbf{r}, \mathbf{s})=\sum_{\mu=0}^{4} v_\mu{}^B(r)\, p_\mu(\hat{r}\cdot\hat{s}), \tag{44}$$

where

$$v_0{}^B(r)=v_0{}^W(r)B(r)+v_{LR0}(r),$$
$$v_2{}^B(r)=v_2{}^W(r)B(r)+v_{LR2}(r),$$

and

$$v_4{}^B(r)=v_4{}^W(r)B(r), \tag{45}$$

which of course reduces to Eq. (39) when $B=0$. Cross sections for several choices of B have been calculated, and it is found that positive values of B yield total cross sections which are even larger at low energies. On the other hand, negative values of B, which have the effect of deepening the potential in the region $r<\frac{1}{2}s$, result in smaller s-wave elastic cross sections and, hence, smaller total cross sections at low energies. The cross sections are only slightly changed at higher energies. In Fig. 6, total cross sections for $j=0$ are illustrated for $R=1.8$ a_0, $B=0$, -2.0, -2.5, and -3.0 a_0^{-1}; and $R=2.0$ a_0, $B=0$, -2.5, and -3.0 a_0^{-1}. Considering the partial cross sections $\sigma_l(0, 0)$, which are illustrated in Fig. 7, we find that the $s\rightarrow s$ contribution $\sigma_0(0, 0)$, which dominates the elastic cross section at low energies, is quite sensitive to B in this low-energy region and becomes independent of B at higher energies. The $p\rightarrow p$ contribution $\sigma_1(0, 0)$, however, is rather insensitive to B for all energies considered. This insensitivity is reflected in the inelastic cross section, which for the transition $0\rightarrow 2$ is given in Fig. 8 for the two values of $R=1.8$ and 2.0 a_0 and choices of $B=0$ and -3.0 a_0^{-1}. For a given value of R, the cross sections for $B=-2.0$ a_0^{-1} and $B=-2.5$ a_0^{-1} are found

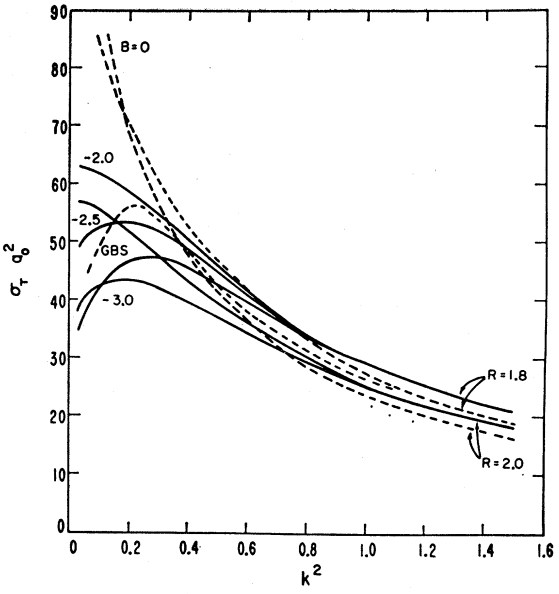

FIG. 6. Comparison of the measured total cross section of Golden, Bandel, and Salerno (GBS) with the calculated $j=0$ total cross section using the unmodified interaction ($B=0$ a_0^{-1}; $R=1.8$, 2.0 a_0) and the modified interaction ($B=-2.0$, -2.5, -3.0 a_0^{-1}; $R=1.8$ a_0 and $B=-2.5$, -3.0 a_0^{-1}; $R=2.0$ a_0).

to lie between the 0 and -3.0 curves, as is expected. Clearly, the effect on the rotational excitation of shifting the low-energy elastic cross section up and down in the manner discussed above is negligible.

We have established, then, that the low-energy elastic scattering can be varied considerably without affecting the rotational excitation; and we recall that in varying R we are adjusting the p-wave scattering to fit the total observed cross section. Since the s-wave scattering is insensitive to R at energies above a few electron volts, it is quite reasonable to conclude that values of R in the neighborhood of 1.8 to 2.0 a_0 best determine the potential as seen by the p-wave function and hence yield the most reliable rotational-excitation cross sections which can be obtained from such a static-field treatment. We have in this investigation examined the sensitivity of the low-energy elastic-scattering cross section to variations in the short-range part of the interaction potential finding that negative values of B, which enhance the interaction in the region $\frac{1}{2}s$, are required in order to obtain reasonable low-energy results. Such a distortion of the short-range static field is probably rather unrealistic. More likely, this is an attempt, with a static-field model, to compensate for the effects of exchange with the bound electrons.

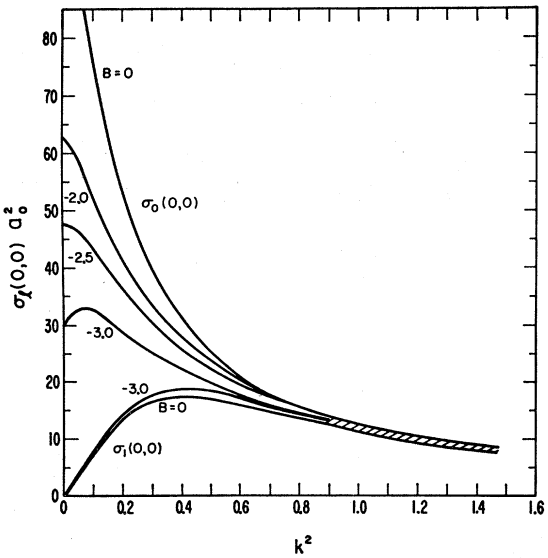

FIG. 7. Comparison of the sensitivity of the $j=0$ elastic s- and p-wave partial cross sections (in a_0^2) to the parameter B in a_0^{-1} ($B=0$, -2.0, -2.5, -3.0, $l=0$ and $B=0$, -3.0; $l=1$) introduced in the modified interaction potential.

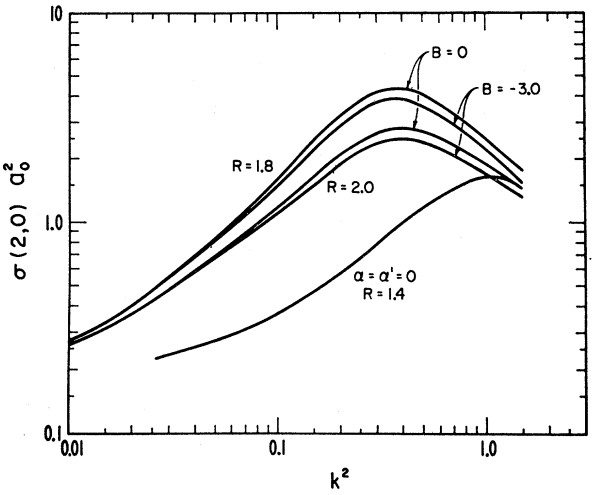

FIG. 8. Calculated values of the rotational excitation cross section $\sigma(2, 0)$ versus energy (in rydberg units) for the cases $B=0$ ($R=1.8$, 2.0, and $R=1.4$, $\alpha=\alpha'=0$) and $B=-3.0$ ($R=1.8$, 2.0), (B in a_0^{-1} and R in a_0).

Massey and Ridley,[16] in their variational treatment of s-wave elastic scattering of electrons from hydrogen molecules, found exchange to be extremely important at energies below 5 or 6 eV, the static-field results being much too large for these low energies. The effect of exchange on p-wave scattering in H_2 has not yet been investigated. However, for all the energies considered in the present static-field investigation, we find that the p-wave elastic cross sections are dominated by the long-range quadrupole and polarization interactions, the short-range interactions playing only a minor role [we have compared values of the partial cross section $\sigma_1(0, 0)$ for $R=\infty$ with the results given in Fig. 4].

TABLE III. H_2 cross sections $\sigma(j',j)$ and $\sigma_T(j)$ in units of a_0^2 for the case $R=1.8\ a_0$ and $B=-2.5\ a_0^{-1}$ (see Ref. 33).

j',j \ k^2 (Ry)	0.004	0.006	0.008	0.01	0.03	0.09	0.15	0.3	0.6	0.9	1.2	1.5
0, 0	40.997	42.610	43.811	44.766	49.110	51.259	51.218	48.338	37.613	29.276	23.693	19.814
2, 0	0.124	0.208	0.255	0.293	0.565	1.479	2.526	4.232	3.810	2.814	2.188	1.803
4, 0	···	···	···	···	3.65(−6)	3.66(−5)	1.200(−4)	5.26(−4)	1.24(−3)	1.57(−3)	1.79(−3)	2.02(−3)
Total 0	41.121	42.818	44.066	45.059	49.675	52.738	53.744	52.570	41.424	32.091	25.882	21.619
1, 1		42.741	43.952	44.916	49.358	51.874	52.252	50.044	39.137	30.401	24.569	20.536
3, 1		0.051	0.103	0.133	0.314	0.864	1.491	2.526	2.284	1.690	1.314	1.082
5, 1		···	···	···	1.4(−6)	1.90(−5)	6.38(−5)	2.88(−4)	6.87(−4)	8.71(−4)	9.91(−4)	1.12(−3)
Total 1		42.791	44.055	45.049	49.672	52.738	53.743	52.570	41.422	32.091	25.883	21.618
2, 2					49.287	51.701	51.955	49.558	38.704	30.082	24.319	20.329
4, 2					0.253	0.719	1.260	2.155	1.958	1.449	1.125	0.928
0, 2					0.134	0.318	0.527	0.859	0.763	0.563	0.438	0.360
Total 2					49.674	52.738	53.742	52.572	41.424	32.094	25.882	21.617
3, 3					49.273	51.663	51.900	49.463	38.608	29.995	24.230	20.236
5, 3					0.210	0.648	1.149	1.985	1.810	1.340	1.043	0.858
1, 3					0.179	0.414	0.683	1.104	0.975	0.716	0.553	0.452
Total 3					49.662	52.725	53.732	52.552	41.393	32.051	25.826	21.546

TABLE IV. H_2 cross sections $\sigma(j',j)$ and $\sigma_T(j)$ in units of a_0^2 for the case $R=2.0\ a_0$ and $B=-2.5\ a_0^{-1}$ (see Ref. 33).

j',j \ k^2 (Ry)	0.004	0.006	0.008	0.01	0.03	0.09	0.15	0.3	0.6	0.9	1.2	1.5
0, 0	49.600	51.181	52.316	53.186	56.383	55.030	52.110	45.290	33.814	26.040	20.924	17.390
2, 0	0.121	0.203	0.248	0.281	0.499	1.097	1.693	2.642	2.634	2.158	1.807	1.570
4, 0	···	···	···	···	3.(−6)	2.79(−5)	8.07(−5)	3.17(−4)	7.81(−4)	1.06(−3)	1.27(−3)	1.49(−3)
Total 0	49.721	51.384	52.564	53.467	56.882	56.127	53.803	47.932	36.448	28.199	22.731	18.960
1, 1		51.307	52.450	53.326	56.602	55.484	52.801	46.354	34.868	26.905	21.647	18.019
3, 1		0.050	0.0995	0.128	0.279	0.642	1.000	1.577	1.579	1.296	1.084	0.943
5, 1		···	···	···	1.31(−6)	1.45(−5)	4.31(−5)	1.73(−4)	4.32(−4)	5.85(−4)	7.04(−4)	8.27(−4)
Total 1		51.357	52.550	53.454	56.881	56.126	53.801	47.931	36.447	28.201	22.731	18.962
2, 2					56.539	55.353	52.603	46.050	34.568	26.657	21.441	17.840
4, 2					0.221	0.536	0.845	1.345	1.352	1.110	0.929	0.807
0, 2					0.117	0.235	0.352	0.537	0.528	0.433	0.361	0.315
Total 2					56.877	56.124	53.800	47.932	36.448	28.200	22.731	18.962
3, 3					56.526	55.325	52.563	45.989	34.494	26.583	21.363	17.756
5, 3					0.187	0.484	0.772	1.237	1.250	1.027	0.862	0.747
1, 3					0.155	0.305	0.454	0.688	0.672	0.548	0.457	0.396
Total 3					56.868	56.114	53.789	47.914	36.416	28.158	22.682	18.899

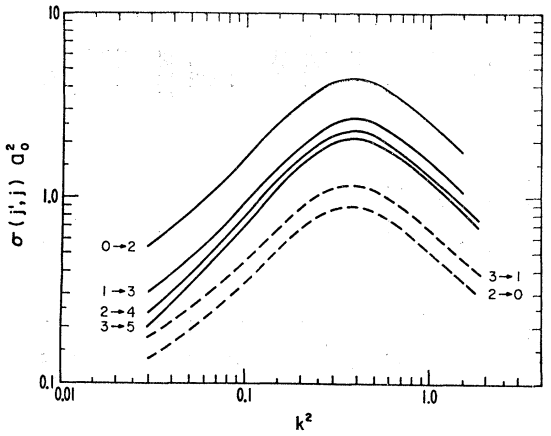

FIG. 9. Calculated values of the inelastic cross section $\sigma(2, 0)$, $\sigma(0, 2)$, $\sigma(3, 1)$, $\sigma(1, 3)$, $\sigma(4, 2)$, and $\sigma(5, 3)$ versus energy (in rydberg units) for the case $B=-2.5\ a_0^{-1}$ and $R=1.8\ a_0$.

Now, since exchange is also expected to behave somewhat like a short-range interaction, we might expect its effect on the p-wave elastic cross section and the rotational excitation cross section to be small. There is some similarity between the short-range character of the electron-H_2 scattering problem and the electron-helium case, where exchange is found to be important to p-wave scattering.[32] However, even with exchange included, the p-wave partial cross sections for helium are found to be an order of magnitude smaller than our (static field) results for H_2. Therefore, if we wish to estimate the exchange correction for H_2 by considering the helium analogy, we must still conclude that the effect is small.

In Tables III and IV are given all cross sections associated with the $j=0$, 1, 2, and 3 states for the two values $R=1.8$ and 2.0 a_0 and $B=-2.5\ a_0^{-1}$. The inelastic cross sections[33] for $j\rightarrow j\pm2$ are illustrated in Fig. 9 and those for $j\rightarrow j+4$ in Fig. 10, along with curves for other R values in the latter case.

Note added in proof. It should be pointed out that a relatively large discrepancy still exists between the theoretical rotational-excitation cross sections $\sigma(2, 0)$ and the results of swarm experiments of Engelhardt and Phelps[7] at liquid-nitrogen temperatures. However, a recent comparison of theoretical and experimental cross sections $\sigma(2, 0)$ carried out by Crompton and McIntosh [R. W. Crompton and A. I. McIntosh, Phys. Rev. Letters, **18**, 527 (1967), and private communication] using their accurate measurements of D/μ, indicates that the theoretical cross sections presented in this paper agree with the measurements within the experimental error.

The $j\rightarrow j+4$ cross sections were found to be quite insensitive to changes in B. The relative contributions of different cross sections to the total electron-scattering cross section for the $j=0$ rotational state are given in Fig. 11. The rotational-excitation cross section $\sigma(2, 0)$ is seen to contribute less than 10% to the total, while $\sigma(4, 0)$ is completely negligible by comparison and is not included.

We have also obtained elastic and rotational-excitation cross sections for D_2. In Table V are given cross sections[33] associated with the rotational states $j=0$, 2, 4 for $R=1.8$ and 2.0 a_0 and $B=-2.5\ a_0^{-1}$. The calculations for D_2 differ from those of H_2 only in the value of the rotational constant. We have used for B_0 (in atomic units, a.u.), the values 2.7×10^{-4} and 1.4×10^{-4} for H_2 and D_2, respectively.

Since all previous calculations[2–6,9–15] of electron scattering from diatomic molecules have involved weak-coupling techniques such as the method of distorted waves or the Born approximation, it is instructive to consider the reliability of such methods in the H_2 problem. By setting certain matrix elements to zero, one can calculate distorted-wave (DW) and Born-approximation (B) results within the framework of

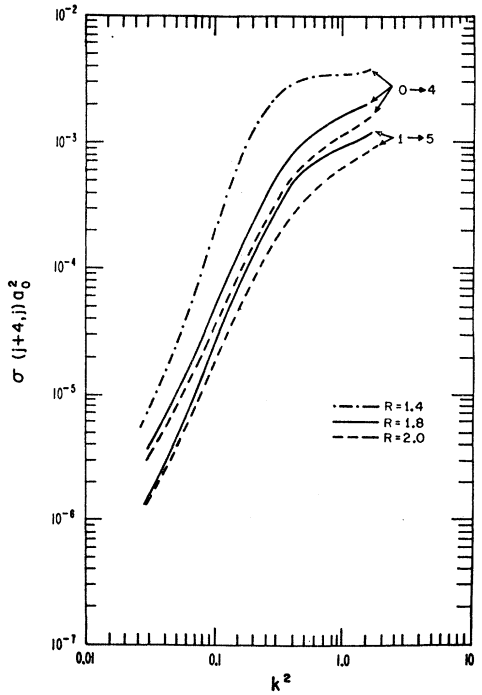

FIG. 10. Calculated values of the inelastic cross sections $\sigma(4, 0)$, using $B=-2.5\ a_0^{-1}$, $R=1.4$, 1.8, and 2.0 a_0, and $\sigma(5, 1)$ using $B=-2.5\ a_0^{-1}$, $R=1.8$ and 2.0 a_0 versus the energy (in rydberg units).

[32] P. M. Morse and W. P. Allis, Phys. Rev. **44**, 269 (1933).

[33] For energies much below $k^2\approx0.01$, the rotational excitation cross sections given here may be expected to be somewhat too small due to our inability to carry the solutions out to values of r large enough to obtain the entire contribution to the R matrix. This accounts for the fact that in Fig. 13 our results seem to lie below the Dalgarno-Moffett curve just above threshold.

the coupled equations. Such calculations for the rotational-excitation cross section $\sigma(2, 0)$ are compared in Fig. 12 with results of the close-coupling calculation (CC) for the case $R=1.8\ a_0$ and $B=-2.5\ a_0^{-1}$; these cross sections are all calculated using the same interaction potential. Just above threshold (not shown) the B, DW, and CC results agree quite well; this is simply an illustration of the fact that at low energies the principal contribution to the rotational-excitation cross section comes from regions far removed from the strong, short-range interaction. At slightly higher energies the distortion of the wave function in the field of the molecule begins to be important. This has the effect of altering the trajectory of the electron, causing it to come closer to the molecule where it can exert a greater torque and hence have an increased probability of causing a change in the angular momentum. Analogously, one can say that taking distortion into account has the effect of drawing the continuum wave functions in closer to the molecule, where they can overlap more strongly with the anisotropic part of the interaction potential, thereby giving rise to a larger cross section for rotational excitation. The effect of including the "back coupling" and coupling to higher states is seen to be considerably smaller, the difference being $<10\%$ for energies below $k^2=0.03$ Ry (0.4 eV) and $<20\%$ for all energies considered. (By back coupling we mean the influence of the inelastic channel on the elastic channel.) In comparing the DW results with those obtained in the close-coupling calculation with $N=2$ and $N=3$, we conclude that the back coupling and the coupling to higher rotational states are of about equal importance for all energies. We did find, however, that the elastic cross section for energies below a few electron volts was quite sensitive to the presence of coupling with an inelastic channel. For example, we found for the case

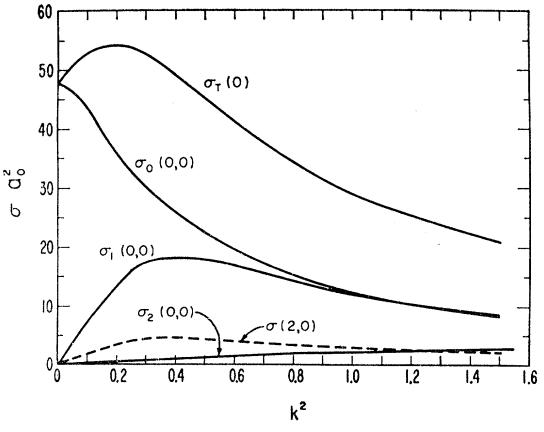

FIG. 11. Calculated values of the elastic partial cross sections $\sigma_0(0, 0)$, $\sigma_1(0, 0)$, and $\sigma_2(0, 0)$, the rotational excitation cross section $\sigma(2, 0)$, and the total cross section $\sigma_T(0)$ for scattering in the $j=0$ rotational state, versus the energy (in rydberg units) for the case $B=-2.5\ a_0^{-1}$ and $R=1.8\ a_0$.

TABLE V. D_2 cross sections $\sigma(j', j)$ and $\sigma_T(j)$ in units of a_0^2 for the case $R=1.8$ and $2.0\ a_0$, $B=-2.5\ a_0^{-1}$ (see Ref. 33).

k^2 (Ry) / j', j	0.003	0.005	0.007	0.009	0.03	0.09	0.15	0.3	0.6	0.9	1.2	1.5
						$R=1.8$						
0, 0	39.917	41.860	43.242	44.306	49.105	51.255	51.210	48.322	37.605	29.272	23.692	19.813
2, 0	0.174	0.237	0.294	0.326	0.593	1.507	2.553	4.245	3.810	2.815	2.189	1.802
4, 0	...	...	...	...	4.8(−6)	4.13(−5)	1.291(−4)	5.443(−4)	1.259(−3)	1.583(−3)	1.797(−3)	2.027(−3)
Total	40.091	42.097	43.536	44.632	49.698	52.762	53.763	52.567	41.416	32.089	25.883	21.617
						$R=2.0$						
0, 0	48.513	50.452	51.780	52.769	56.377	55.025	52.104	45.281	33.808	26.037	20.923	17.389
2, 0	0.172	0.232	0.285	0.313	0.523	1.116	1.709	2.651	2.635	2.159	1.808	1.570
4, 0	...	...	...	...	4.(−6)	3.12(−5)	8.643(−5)	3.273(−4)	7.918(−4)	1.064(−3)	1.272(−3)	1.498(−3)
Total	48.685	50.684	52.065	53.082	56.900	56.141	53.813	47.932	36.444	28.197	22.732	18.960

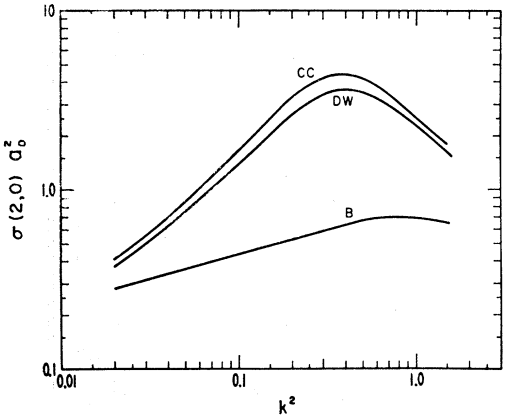

FIG. 12. Calculated values of the rotational excitation cross section $\sigma(2,0)$ using the close-coupling (CC), distorted-wave (DW), and Born approximation (B) methods for the case $B=-2.5\ a_0^{-1}$ and $R=1.8\ a_0$.

$R=1.8\ a_0$ and $B=-2.5$, that the s-wave elastic cross section for scattering in the $j=0$ state was reduced from 60.7 a_0^2 to 47.1 a_0^2 at $k^2=0.03$ Ry by including coupling with the $j=2$ state. Thus, it is clear that for energies above the threshold for rotational excitation, a *one-state* calculation of the elastic cross section may be very misleading. Similarly, a potential obtained by fitting such a cross section to observed low-energy results may be poorly determined.

In Fig. 13 we have compared our results (LG) for the $j=0\rightarrow 2$ rotational-excitation cross section[33] ($B=-2.5$) with the results of other authors. We recall that the Gerjuoy and Stein (GS) cross sections[5,6] are calculated by applying the Born approximation to the pure quadrupole interaction. Dalgarno and Moffett (DM)[9] include the effects of polarization and obtain a somewhat larger cross section. The effects of distortion are included in the calculations of Dalgarno and Henry (DH),[15] Mjolsness and Sampson (MS),[11] and Geltman and Takanayagi (GT).[13,14] Dalgarno and Henry,[15] using the molecular wave functions of Hagstrom and Shull, obtain analytic expressions for the appropriate interaction matrix elements and calculate rotational-excitation cross sections by the method of distorted waves. While their interaction matrix elements do include the long-range effect of the quadrupole moment, no allowance is made for the *effective* polarization interaction, which is thought to be important.

Mjolsness and Sampson[11] do not attempt to accurately represent the short-range field, but rather rely on the importance of the long-range field at low energies. They include polarization by cutting off the asymptotic potential by means of an exponential cutoff (MS a) similar to our $C(r)$ of Eq. (38), or a nonexponential cutoff (MS b) which corresponds to replacing r^4 by $(r^2+R^2)^2$ in the polarization part of Eqs. (36) and (37). They also include the quadrupole interaction by cutting off the quadrupole part of Eq. (37) sharply at r_c (we have included, in Fig. 13, their results for the choice of $r_c=a_0$). An appropriate value of R is then obtained by fitting the calculated momentum-transfer cross section to the results of swarm experiments[7] for energies up to 1 eV. The principal objection to this approach, as was discussed in Sec. I, is the fact that s-wave scattering, which dominates the elastic and momentum-transfer cross sections at low energies, is sensitive to variations in the interaction potential which have very little effect on the p-wave functions, which principally determine the rotational-excitation cross section. Thus, an adjustment of the interaction potential in regions which do influnece p-wave scattering, in order to make up, possibly, for a failure to accurately represent the short-range fields or to allow for the effects of exchange, appears to be somewhat unreliable.

In the work of Geltman and Takayanagi,[14] the nonspherical part of the short-range field $v_2(r)$ is calculated by representing the molecular charge distribution by that of two hydrogen atoms placed a distance s apart. The resulting potential is not very much different from those potentials in Fig. 2. The long-range polarization and quadrupole interactions are similarly included by cutting off the asymptotic form of Eqs. (36) and (37) [with $C(r)=1$] at $r=R$. The nonspherical part is then smoothly taken to zero, while the spherical part is assigned the value $-\alpha/2R^4$ for $r<R$. The cutoff parameter R is then determined by fitting the calculated elastic cross section to observed total scattering cross sections out to 7 eV or so. In attempting to fit observed total cross sections above the thresholds for rotational and vibrational excitation, one must be careful to consider the inelastic cross sections which also contribute. In the case of hydrogen, however, these cross sections are thought to be small relative to the elastic

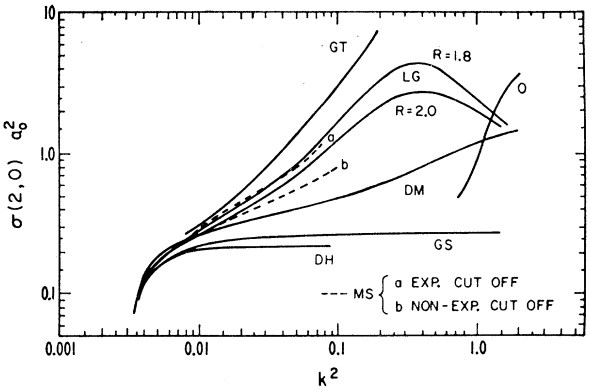

FIG. 13. Comparison of the rotational excitation cross section $\sigma(2,0)$ calculated in this work (for the case $B=-2.5\ a_0^{-1}$; $R=1.8$ and 2.0 a_0) with the results of other authors (see Ref. 33): (LG) present work, (GT) Geltman and Takayanagi, Ref. 14, (MS) Sampson and Mjolsness, Ref. 11, (DM) Dalgarno and Moffett, Ref. 9, (GS) Gerjuoy and Stein, Refs. 5, 6, (DH) Dalgarno and Henry, Ref. 15, (O) Oksyuk, Ref. (27).

cross section.[8,31] The curve (GT) given in Fig. 13 results from a choice[14] of $R=1.2\ a_0$ and corresponds to an elastic cross section given in Fig. 3 of Ref. 13. In attempting to keep the elastic cross section down to reasonable values for lower energies, Geltman and Takayanagi chose the value of $R=1.2\ a_0$ which includes more polarization than in our calculation (LG), and which results in a somewhat larger rotational-excitation cross section.

Oksyuk (O)[27] applied the adiabatic approximation to rotational and vibrational excitation of diatomic molecules, using the interaction potential derived by Fisk,[26] which ignores the polarization and quadrupole long-range interactions. Comparing this curve with our result for the case $\alpha=\alpha'=0$ and $R=\infty$ (Fig. 5) suggests quite similar behavior for energies $k^2\lesssim 1.0$ Ry. For larger energies, however, the Oksyuk cross section becomes larger than any of our results. Comparing the interaction potentials given in Figs. 1 and 2, we are inclined to conclude that this difference in the high-energy behavior of the cross sections is due not to differences in the short-range interaction potentials, but rather to differences in the methods of determining the cross sections. In any case, we feel that the failure to include the long-range interactions results in rotational-excitation cross sections much too small for all energies below $k^2=1.0$ Ry.

For heavier molecules such as O_2 and N_2, which are of great interest in connection with swarm experiments,[8] the electron-molecule interaction potentials are much larger than in the case of H_2, and we expect the weak-coupling methods to be correspondingly poorer. The breakdown of the method of distorted waves, for instance, is apparent in the work of Geltman and Takayanagi.[14] In such cases, the approach illustrated by the present work must be used.

ACKNOWLEDGMENTS

The authors would like to thank Mrs. Joni Sue Lane for her assistance in writing all the computer codes used in the calculations. One of us (N.F.L.) wishes to express his gratitude to Dr. Roy H. Garstang and the other staff members of the Joint Institute for Laboratory Astrophysics for their hospitality during his stay as a visiting fellow.

Experimental Evidence for Xe_2 Molecules*†

SHARDANAND‡

Department of Geology and Geophysics and Research Laboratory of Electronics, Massachusetts Institute of Technology, Cambridge, Massachusetts

(Received 23 January 1967)

Using the standard absorption-measurement technique, we have measured the attenuation cross sections at Lyman-α (1215.7 Å) for xenon. The attenuation does not follow Beer's law. The observed linear increase in attenuation cross section with rise in gas pressure, and the related decrease in attenuation cross section with increase in temperature, are ascribed to the formation of Xe_2 molecules. From consideration of diatomic molecules, methods are presented for deriving the photon scattering cross section for atomic species, the equilibrium constant for the reaction $Xe+Xe\rightleftarrows Xe_2$, the absorption cross section, and the heat of dissociation for Xe_2. Their respective values were found to be 5×10^{-22} cm^2, 2.16×10^{-22} cm^3/molecule, 1.85×10^{-17} cm^2, and 0.03 ± 0.001 eV.

I. INTRODUCTION

MEASUREMENTS of the relative scattering cross sections for He, Ne, H_2, Ar, and N_2, by observing the right-angle scattering have been previously reported by Shardanand and Mikawa.[1] These investigations have been extended by the present author for Xe and Kr by measuring C/Φ values as a function of pressure.[1] These preliminary unpublished measurements have established the fact that the derived relative cross sections for Xe and Kr are at least one order of magnitude less than similar results of Gill and Heddle.[2] It may be recalled that Gill and Heddle have pointed out that since the resonance lines for Xe and Kr lie within the sensitive wave band of their photon counter, their measured values for these two gases could be too high. In our investigation, the sensitive wave band was defined by the oxygen filter that reduced the error re-

* This work was supported by the National Aeronautics and Space Administration while the author was with GCA Corporation, Bedford, Massachusetts.

† This work was supported in part by the National Aeronautics and Space Administration (Contract No. NAS12-436) while the author was at the Research Laboratory of Electronics, M.I.T.

‡ Present address: NASA Electronics Research Center, Cambridge, Massachusetts.

[1] Shardanand and Y. Mikawa, J. Quant. Spectry. Radiative Transfer (to be published); see especially Eq. (2).

[2] P. Gill and D. W. O. Heddle, J. Opt. Soc. Am. **53**, 847 (1963).